Sustainable Energy Technologies and Assessments 53 (2022) 102458

Contents lists available at ScienceDirect

Sustainable Energy Technologies and Assessments

journal homepage: www.elsevier.com/locate/seta

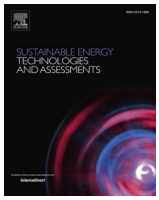

Original article

Fluidized bed gasification of biomass from plant-assisted bioremediation: Fate of contaminants

Francesco Gallucci [a], Enrico Paris [a], Adriano Palma [a], Beatrice Vincenti [a], Monica Carnevale [a], Valeria Ancona [b], Domenico Borello [c,*]

[a] CREA, Italy
[b] Istituto di Ricerca Sulle Acque del Consiglio Nazionale delle Ricerche, Bari, Italy
[c] Dipartimento di Ingegneria Meccanica e Aerospaziale, Università di Roma La Sapienza, Italy

ARTICLE INFO

Keywords:
Fluidized bed gasification (FBG)
Heavy metals (HMs)
Polychlorinated biphenyls (PCBs)
Volatile organic compounds (VOCs)
Plant-assisted bioremediation (PABR)
TGA-DTA

ABSTRACT

Fluidized-bed gasification (FBG) of Phyto-assisted Bioremediation (PABR) biomass is analyzed focusing on the contaminants' dispersion. Poplar pruning coming from an area contaminated by polychlorinated biphenyls (PCBs) and heavy metals (HM) are considered. The biomass analysis showed relevant contents in HMs, especially Cd and Cr, and no significant PCB content. FBG process was analyzed to: a) track pollutants, b) detect contaminants in the FBG and c) investigate the HMs concentration in the produced streams. The results showed that most of the metals are concentrated in the ashes collected in the bottom of the reactor (Pb, Cd, Cu, Cr), or in the cyclone (B, Na, Mg, Al, K and Fe). Interestingly, metals are also released by the olivine bed (Mg, Fe, Ni and Al) and transported downstream. Consistent fractions of Zn and Fe (also Cu) were detected in the fugitive ashes. As for the Volatile Organic Compounds (VOC) concentration, we noted similarities between PABR and virgin biomass syngas streams. A reduced-scale process was carried out in TGA-DTA to investigate the potential of such technique in reproducing the main features of the FBG process. Comparable results were obtained, thus suggesting its possible application for small-scale preliminary assessment of FBG process.

Introduction

The quest for an increasing exploitation of renewable energy sources (RES) and a reduction of greenhouse gas emissions-GHG emissions in the production of heat and electricity, has boosted the development of wind, solar and bioenergy technologies [1]. Among the available RES, bioenergy represents an environmentally friendly and carbon–neutral solution with worldwide availability. This led to a growing interest in the production of sustainable liquid and gaseous fuels such as green hydrogen, renewable methane, and other chemicals. The use of such fuels can support the reaching of the EU targets for 2030, when the GHG should be reduced to at least 40% if compared with 1990 and it is targeted an increase of the energy efficiency of 32.5%. At the end of June 2021, the EU launched a more ambitious program named Fit for 55 in which the GHG reduction (from 1990 values) was increased to 55%. The share of renewable energies in the energy consumption is required to reach 32% in 2030 [2]. In 2018, biomass and other bio-energies provided more than 50% of the worldwide renewable energy consumption [1]. Biomass production requires the use of fertile soils. Unfortunately, such cultivations compete with crops and will eventually lead to the exploitation and conversion of arable land and will promote deforestation [3]. To favor the exploitation of biomass as renewable energy source while maintaining sustainability, the use of residual biomass (i.e., by-products of other processes or cultivated in marginal lands) can be advantageously considered as a resource. Phyto-technologies, that are employed for the recovering of polluted soils and producing biomass, can be an attractive solution. For example, in Italy, 0.57% of the entire soil extension is mapped as contaminated. In 39 "sites of national interest" (SIN) [4] various actions are underway for the mapping and recovery of contamination. Among several possible actions, plant-assisted bioremediation (PABR) stands for a sustainable strategy to recovery contaminated soils. Plant species and soil microorganisms act synergistically to promote the transformation of contaminants into less toxic compounds therefore, to clean up the soil from pollution [5]. Ruthens et al. [6], reported on the implementation of a phytoremediation strategy on a soil contaminated by heavy metals in Belgium. By using willows

* Corresponding author.
E-mail addresses: francesco.gallucci@crea.gov.it (F. Gallucci), enrico.paris@crea.gov.it (E. Paris), adriano.palma@crea.gov.it (A. Palma), beatrice.vincenti@crea.gov.it (B. Vincenti), monica.carnevale@crea.gov.it (M. Carnevale), valeria.ancona@ba.irsa.cnr.it (V. Ancona), domenico.borello@uniroma1.it (D. Borello).

https://doi.org/10.1016/j.seta.2022.102458
Received 25 November 2021; Received in revised form 7 June 2022; Accepted 18 June 2022

and poplars, they showed a survival rate of 91% of the planted trees and they indicated an average production rate of biomass of 1.5–9 ton DW (dry weight) of biomass per ha and per year. Even if their results indicated that at least 36 years were needed to reduce Cd to legal limits, they demonstrated a linear extraction rate and a clean-up depth of 50 cm. Giudicianni et al. [7] carried out several investigations in South of Italy and were able to demonstrate that it is possible to produce 13 ton/ha/y of biomass from multi-contaminated soils, thus suggesting interesting applications for distributed generation of heat and power in local areas when using the produced biomass. Fiorentino et al. [8], evaluated the possibility to use giant reed for energy use together with pollutants phytoextraction and restauration of soil fertility. The experiments lasted two years in soil from the ILVA brownfield site located in the South of Italy (Campania Region). They found a growth rate of giant reed lowered by 16% compared to the case of non-polluted soil. However, giant reed was able to produce interesting amounts of ligno-cellulosic biomass with low levels of potentially toxic materials. The soil at the end of the testing period revealed a reduction in Pb and Zn concentrations. As known, the biomass treatment generates different products: solid (char, ashes, metals), volatile, semi-volatile such as tar, volatile organic compounds (VOCs) and gaseous (syngas). Compared with virgin biomass, PABR biomass can be characterized by the presence of several contaminants (e.g., heavy metals, traces of polychlorinated biphenyls, dioxins, etc.) that are extracted from the soil and need to be safely disposed. In the last years, the research group investigated the property of biomass obtained from PABR applications [9]. Biomass was widely analyzed, as its quality needs to be investigated and verified before considering the possibility to use it for energy purposes. The main interest in the analysis is focused on the detection of pollutants released in the PABR biomass treatment. A variety of metals could be stored in PABR biomass, and this circumstance introduces some uncertainties about the implementation of a safe procedure for the use of such biomass in energy valorization processes. In fact, depending on the volatility of the metals considered, it is possible to find them in the bottom, flying, or eventually in the fugitive ashes mixed with the gaseous effluents. Some studies described the effectiveness of different contaminated biomass treatments, i.e., combustion and gasification [9–13]. Keller et al. [11], analyzed a process for removing metals from the incineration ashes by implementing a procedure based on tube furnace with a thermo-desorption device. They measured on-line the metals volatilization while varying the temperature with a constant rate. By increasing the temperature, the released elements were (in order): Cd, K, Na, Zn. This suggests that, when heavy metals concentration is known, it is possible to set the proper operating temperature to volatilize metal components aiming at concentrating target metals in specific location inside the gasifier. Other treatments were tested for studying the possible utilization of biomass from PABR strategy. Among these, pyrolysis tests were carried out by different authors with the aim to discover energy production capability [14–17]. Several studies were carried out to assess, also numerically, the energy use of biomass in combustion [18] as well as in pyrolysis/gasification [19,20] processes. The gasification process [21] represents a very interesting approach for producing syngas from biomass with a very efficient conversion process (the syngas low heat value -LHV- is about 75% of the solid biomass) and with the possibility to upgrade the syngas with specific treatments aiming at increasing H_2 content (water gas shift) and/or reducing CO_2 emissions. Among the different available gasification technologies, fluidized bed gasification (FBG) offers the decisive advantage of a constant bed temperature that can be enforced during the process thanks to the bubbling of the bed, constituted by suitable selected materials (e.g., olivine, K-Feldspar, quartz sand [22]) as well as biomass, that allows to strictly control the conversion process. Rapagnà et al. [23], analyzed a configuration with a FBG operating with olivine and dolomite as bed material. Such materials have good catalytic properties due to the presence of iron and were selected aiming at improving the tar reduction [24,25]. The presence of a cyclone and of a ceramic filter downstream of the FBG allowed to properly separate ashes and to improve the cracking of residual tars. Then, gasification seems to represent a possible route for treating PABR biomass aiming at producing a syngas that could be efficiently treated to remove the metals contained in the fugitive ashes before delivering it to the cogeneration unit [9]. Vervaeke et al. [26], analyzed the fate of HMs in a fixed bed downdraft gasifier by using willow PABR biomass. They studied the distribution of the metals present in the biomass into the different gasification streams. In their case, Cr, Cu and Ni were concentrated in the bottom ashes (i.e., the solid residual in the main reactor) while Cd, Pb and Zn were mainly detected in the filtering/purification process applied to the volatile fraction (flying/fugitive ashes). The application of such analysis to other biomass types and other gasification technologies remained unexplored. A fundamental step for these investigations consists in the characterization of biomass and biochar, as well as of the syngas produced during the gasification process. The aim is to validate a proper strategy able to annihilate the emission of hazardous materials (heavy metals – HM - and/or tars). Presently, in Italy, biomass from PABR cannot be used as renewable biomass if it is transported out from the production site. This work has the ambition to constitute a step for the updating of the actual procedure aiming at establishing guidelines for a clean and sustainable use of PABR biomass for energy uses. A pilot bubbling bed gasifier, installed at the Dept. of Mechanical and Aerospace Engineering (DIMA), Sapienza University of Rome, was successfully used for the gasification of several classes of woody biomass (e.g., hazelnut shells [27] and poplar pruning [28]). In [28], the properties of contaminated and virgin poplar pruning are compared with hazelnut shells demonstrating that not many differences are noticeable between the two types of poplars in terms of syngas quality, while some differences were observed when comparing the results with hazelnut shells. Interestingly, a lower content in tars was measured in the gasification of PABR biomass, thus suggesting a possible catalytic effect of the metals present in the reactors, mainly Ni, which remain trapped in the ashes at the bottom of the reactor. Similar effects could be determined by the presence of Ca and K, that have a catalytic action in the char gasification process [29,30]. This could represent a valid alternative to the use of catalytic post-reactors for the tar cracking, [27]. However, a systematic characterization of the HMs dispersion in the streams of FBG was not carried out so far. It is then worth carrying out an in-depth study on the gasification of biomass coming from contaminated sites aiming at assessing a process able to produce high quality, clean syngas as well as to enhance a sustainable remediation strategy for contaminated soils. This step requires the definition of guidelines to track and entrap the dispersed contaminants, to guarantee that the emissions are comparable with those of non-contaminated (virgin) biomass. In this work, a FBG was used for the gasification treatments of PABR biomass. To properly assess the path of the hazardous compounds potentially produced in the gasification process of PABR biomass, an accurate analysis of pollutants (HM and PCBs) and VOCs in syngas, bottom, cyclone, and fugitive ashes, was carried out. We investigated how pollutants are released and in which part of the gasifier they are placed (bottom or fugitive ashes) as well as how such contaminants can be trapped. A complementary TGA-DTA analysis was also carried out trying to mimic the release of metals and VOCs on a small-scale experiment. We defined the distribution of metals according to their distribution between bottom, flying and fugitive ash. The TGA-DTA lab-scale experimental setting was developed as a route to preliminarily determine the emission potential of a contaminated biomass and to test unknown biomass using reduced volumes of material, saving on time and costs of using a gasifier. In the next paragraph, materials and methods, the FBG and the TGA-DTA experiments as well as the sampling and the analysis methodologies are described. Then, the results of the experimental campaign are discussed by focusing on the characteristics of biomass and syngas, as well as the concentration and the distribution of metals and VOCs.

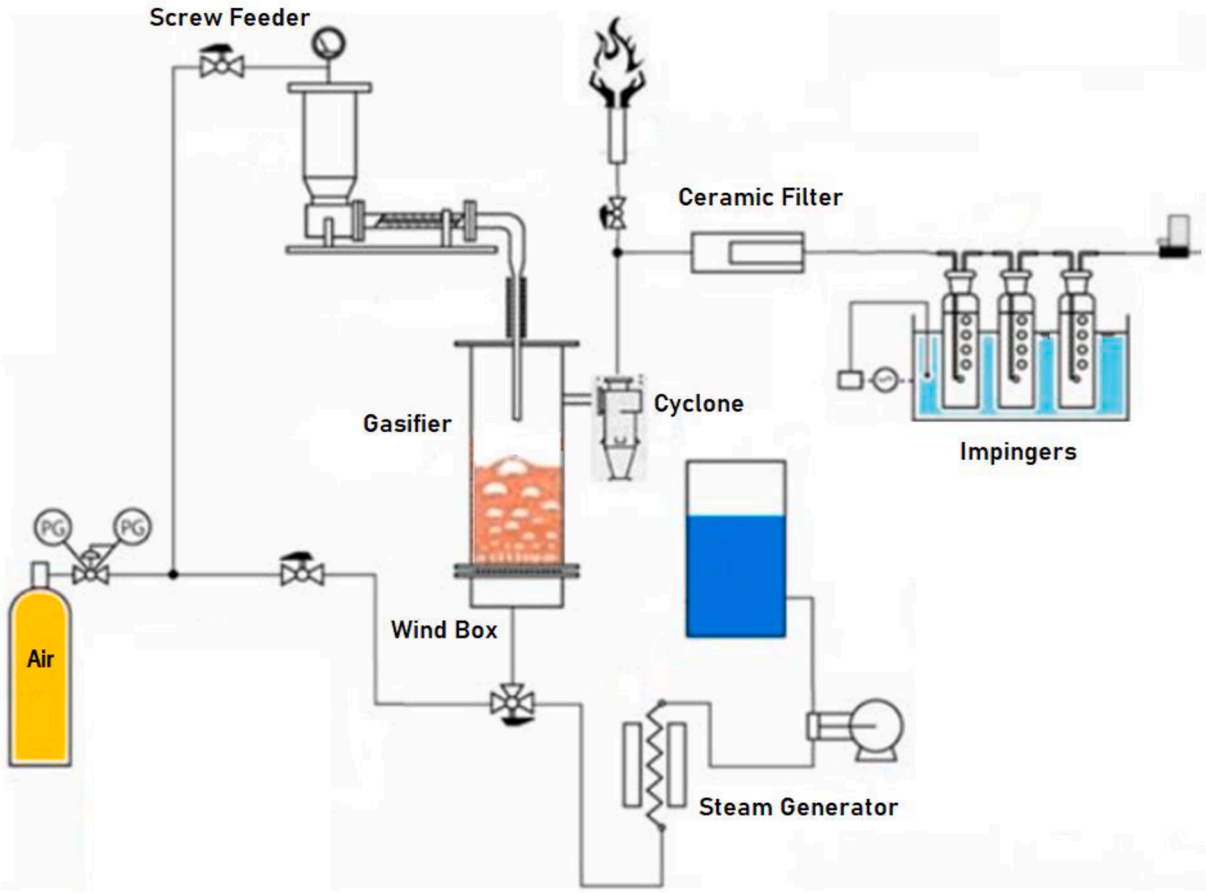

Fig. 1. Diagram of the gasification plant [27,32].

Materials and methods

The biomass used in this study came from a multi-contaminated area located in South of Italy, close to Taranto. Here, since 2013, IRSA-CNR is conducting a PABR action using poplars [31]. In such area, PCBs, as well as some heavy metals (Pb, Zn, Sn, etc.), were dispersed during the previous uncontrolled site management. In previous studies conducted in the same area, Ancona et al. [9,31], assessed the soil and biomass contamination (both HMs and PCBs) and evaluated the quality of the syngas produced over time. The gasification tests here presented were carried out in the FBG located in DIMA – Sapienza (Rome) [27] while the TGA-DTA analysis, biomass characterizations and the other instrumental measurements were performed at LASER-B laboratory of CREA-IT in Monterotondo (RM).

Biomass characterization

Biomass is obtained by the periodic maintenance of two poplar treated areas, in the survey site, when pruning residues are collected and naturally dried. Poplars were planted in 2013 to reduce PCB and HM contamination of soil and to restore soil quality. Scarce amounts of nutrients, low bacterial abundance and cell-viability values were observed in the soil before PABR strategy application [9,31]. Preliminarily, the dried biomass was ground with a Retsch SM 100 knife mill first and subsequently refined using a Retsch ZM 200 centrifugal mill. One gram of biomass sample was placed in the Lenton EF11/8B muffle furnace and heated up to 250 °C for one hour. Then the temperature was raised up to 550 °C for two hours to determine the ash content (UNI EN ISO 18122:2016).

The higher heating value (HHV) was ascertained using an Anton Paar 6400 isoperibol calorimeter. Through a pellet press (Pellet Press 2810) a sample of about 1 g was prepared for each analysis. The calorimeter was always pre-calibrated with benzoic acid analytical standard. The analysis was performed in triplicate (UNI EN ISO 18125:2018). The lower heating value (LHV) was calculated considering the HHV and the hydrogen content. The elemental analysis was performed by *Costech ECS 4010 CHNS-O elemental analyzer* according to UNI EN ISO 16948:2015. The sample was weighed (about 5 mg) into tin capsules and inserted into the reactor. The limit of quantification (LOQ) for each sample was 0.05%w/w. The oxygen content was calculated by difference on dry-based samples (UNI EN ISO 16948:2015). The determination of the metal content was carried out in the biomass by means of inductively coupled plasma mass spectrometry, ICP-MS Agilent 7700 Series. The content of Polychlorinated Biphenyls in poplar pruning biomass samples was evaluated by using a *ThermoElectron TRACE GC Ultra* coupled with a *PolarisQ Ion Trap* (Thermo Electron, Austin, TX) mass spectrometer equipped with a PTV injector and a TriPLUS RSH autosampler. Before the analysis, biomass samples (0.5 gr each one) were extracted in triplicate with an Accelerated Solvent Extractor (ASE 350 DIONEX) in accordance with the procedure described by Ancona et al. [31]. A total of 31 PCB congeners were quantified using a nine-point calibration curve and each congener concentration was indicated as ng of PCBs per g of dry biomass sample. Average values of three replicates were considered for each analysis. On detail, 12 dioxin-like PCBs (81, 77, 105, 114, 118, 123, 126, 156, 157, 169, 167, 189), 6 markers (28, 52, 101, 153, 138, 180) and 13 non-dioxin-like PCBs (18, 44, 95, 99, 110, 128, 146, 149, 151, 183, 187, 170, 177) were investigated. A standard mix solution (LABMIX G31 in isooctane, Lab Instruments) was used for PCB curve calibration and quantification at GC–MS. All biomass characterization tests were conducted in duplicate.

Table 1
Fluxes in the gasifier.

Air	Water/steam	Biomass	Steam-to-biomass	Equivalence ratio
5.9 Nl/min	150 g/h	300 g/h	0.5	0.3

Table 2
Operating temperature in the FBG.

Wind Box	Gasifier	Ceramic Filter	Steam Generator	Thermal Bath
450 °C	820 °C	400 °C	200 °C	9 °C

Gasification plant

The gasification tests were carried out in the fluidized bed reactor facility located at DIMA and previously described in several papers (e.g. [27,28]). The sketch of the plant is shown here for convenience (Fig. 1).

Details of the experimental setup employed for FBG test are described as follows. PABR biomass obtained from pruning of the Taranto poplar treated areas was chipped and then sieved to remove the chips smaller than 0.8 mm. Olivine was used as bed materials in the FBG (Gasifier in Fig. 1). The sand was also sieved to ensure a granulometry ranging between 0.4 and 0.8 mm. The system operated at constant (atmospheric) pressure, with a small overpressure in the fluidized bed of about 200 mbar (20 kPa). The fluids (air and steam) are sent in the FBG from the bottom side and controlled with a mass flow rate to enforce a flux sufficient to generate a bubbling bed as well as to feed the gasifier with enough oxygen and steam to support the gasification reactions [33]. Gasification is favored using steam, which increases the quality of the syngas produced by increasing the H_2 content [27]. Water and air flows are controlled under LabView® by using two mass flow controllers: Bronkhorst miniCORI flow – 0–10 kg/h and Bronkhorst miniCORI flow – 0–100 Nml/min, respectively. A Bronkhorst MFC calibrated for syngas flow in the range between 8 and 400 Nml/min was used for computing the syngas slipstream sent to the impinger bottles where VOCs and metals were measured. A Baggi MCR series – 0–100 Nl/min was used for setting air flow. Biomass is sent in the gasifier through a cochlea (screw feeder) moved by an electric engine and properly calibrated by the authors to control the biomass flow rate by varying the angular velocity. The fluxes of reacting substances are calibrated to obtain proper values of steam-to-biomass and equivalence ratio (Table 1), in agreement with previous studies [9,27,28].

As for the operating temperature, different values were set in the different FBG components (see Table 2). In the fluidized bed where gasification occurs a temperature of 820 °C was set in agreement to [28]. To have a homogeneous temperature distribution of the olivine bed, the system reached the set point an hour before the start of the sampling.

Water is vaporized in the steam generator (at 200 °C to avoid risk of liquefaction) and the air/steam mixture is pre-heated (at 450 °C) in the wind box before entering the main gasification bubbling reactor. In the bubbling reactor, syngas is produced and delivered to the cleaning section through a pipe placed in the top region. On the contrary, most of char and ashes remain trapped in the reactor bed where they mix with olivine. The syngas cleaning section consists in 1) a cyclone to remove the largest char and ashes fractions that are dragged by the gas flow and 2) a ceramic filter where gas is heated up to 400 °C to favor the thermal cracking of heavy compounds while avoiding tar deposit. Finally, syngas passes in the final trapping system for fugitive ashes, tars and metals. The trapping system consists in a series of 3 impingers of 250 ml each, filled with 100 ml of a nitric acid solution that will be described in the following. The bubblers were placed in a thermal bath at 9 °C. The VOCs are captured from the carrier stream with an active sampling system consisting in a cross-flow extraction with a syringe of 100 ml using multi-layers tubes for thermal desorption placed before and after the ceramic filter. All tests were conducted in duplicate.

TGa-DTA

The thermo-gravimetric/differential thermal analyses (TGA-DTA) were performed by using a *Mettler TGA/DSC1 Star* in the following operating conditions: temperature between 25 °C and 800 °C; heating rate 90 °C/min (the upper instrumental limit and therefore the best thermal approximation to the reactor gasification process) and nitrogen flow rate of 60 ml/min for pyro-gasification tests. There are some instrumental limits that make the TGA-DTA process different from a FBG process, above all in terms of biomass feed and temperature achievement rate. However, the results obtained are very satisfactory and innovative with good agreement with (part of) the FBG findings, as it will be shown in the following paragraphs. Indeed, generally the TGA-

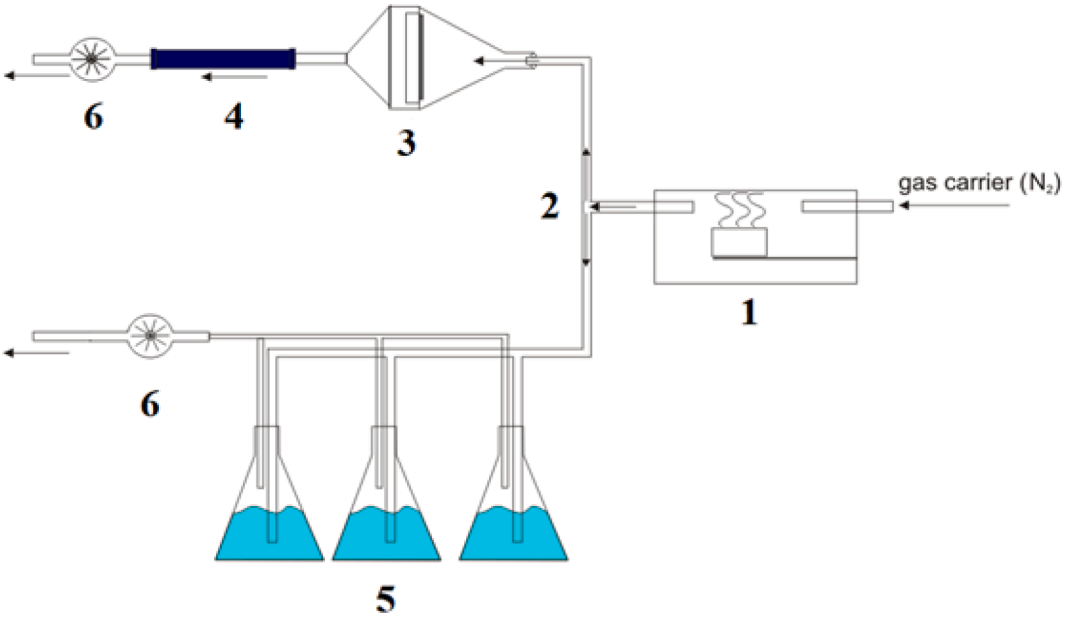

Fig. 2. Experimental sampling system from the TGA-DTA analysis. 1-Furnace, 2-Flow splitting, 3-PM sampler holder, 4-Tube for VOCs sampling, 5-Bubblers for metals sampling, 6-Suction pumps.

Table 3
GC ramp for VOC analysis.

	Rate (°C/min)	T(°C)	Hold time (min)
Initial	–	35	3
Ramp	5	250	5

Table 4
Characterization of PABR poplar pruning residues.

Biomass Characterization	
HHV (MJ/kg)	17.65 ± 0.53
LHV (MJ/kg)	15.21 ± 0.61
C (wt. %)	50.87 ± 1.44
H (wt. %)	11.88 ± 0.94
N (wt. %)	1.06 ± 0.37
S (wt. %)	<LOQ
Ash (wt. %)	2.40 ± 0.21
Total Solid (wt. %)	85.99
Fixed Carbon (wt. %)	10.55
Volatile Matter (wt. %)	73.04

Table 5
Solid residues from poplar pruning gasification.

Components	C (**wt.** %)	H (**wt.**%)	N (**wt.**%)	S (**wt.**%)
Biochar	82.45	4.62	1.78	<LOQ
Ash + biochar	44.91	2.41	1.26	<LOQ

Table 6
Concentration of PCB congeners detected in PABR poplar pruning residues (in ng/g).

Markers *28, 52, 101, 138, 153, 180*	**DX like** *105, 118, 126, 169*	**No DX like** *18, 44, 95, 99, 110,146, 149, 151, 183, 187*
21.85 ± 3.07	4.90 ± 1.14	13.70 ± 1.36

DTA system is used to simulate the behavior of a matrix in combustion and pyrolysis processes (see e.g. [34]). To the best of the authors' knowledge this is the first time that such a system was setup to evaluate the emissions that can be generated. The contemporary sampling of airborne and gas dusts from the TGA-DTA was realized with the experimental setup shown in Fig. 2.

In Fig. 2, the sampling system is shown. A small quantity of biomass (≈5 mg) was placed in a furnace (1). The emissive flow was divided into two parts (2). The first was channeled towards a sampler holder (3) with a 25 mm Ø and 0.49 μm glass wool filter for dust abatement. Filter porosity allowed the passage of gaseous effluents but not of PM, a sampling tube (4) was placed in sequence for the trapping and subsequent thermal desorption of the VOCs. The second flux was channeled towards a series of bubblers (5) containing a solution of $HNO_3 + H_2O_2$ in H_2O MilliQ for capturing metals. To guarantee a constant flow, two suction pumps, properly calibrated, were placed at the end of the system (6). All tests were conducted in duplicate.

VOCs sampling and analysis

ATA tubes (Air toxic analyzer, Markes Int.) were used for the sampling of VOCs. The sampling procedure in the FGB and TGA-DTA is described in the above paragraphs. The sampling was performed in triplicate and a second *backup tube* was placed in series with each sampling tube. The sampling in the TGA-DTA system was carried out by placing the adsorbent tubes after the glass wool filter, so that it could trap the particulate material and let volatile compounds pass through. A pump was placed downstream of the tubes to maintain the constant sampling flow at 60 ml / min. In the FBG plant, 100 ml of syngas were sampled at the reactor exit by using a syringe. The *backup tube* gave recoveries of less than 5% for the sampling here carried out, therefore all the data obtained were considered significant. The analysis was performed with a 100-xr TD (Markes Int.) coupled to an Agilent 7000 GC/MS system. The tubes were thermodesorbed with a flow of 50 ml / min up to a temperature of 350 °C for 10 min in split-less mode. They were collected on focusing trap at the temperature of –22 °C and then was re-desorbed from the focusing trap for 1 min with a 1:10 split. The GC/MS analysis was carried out in split-less mode following the ramp specified in Table 3.

The acquisition was performed in full-scan mode in the *m/z* 35–450 range with an EI ion source at a temperature of 250° C. The recognition of analytes was realized with *MassHunter software* and using NIST library taking into consideration only the data with a match factor over 80%.

Metal sampling and analysis

The metals were sampled in according to the UNI EN 14385. The gaseous effluents bubble within solutions for the sampling. Three glass bubblers (250 ml, DadoLab srl) were used containing a solution of equal volumes of HNO_3 (mass fraction V≈ 65%) and H_2O_2 (mass fraction V≈ 30%), diluted in nine parts of water. The same analytical procedure was applied to the output of the TGA-DTA system. In addition, the flying ashes from the multicyclone were collected, mineralized, and analyzed in ICP-MS. Being unable to analyze the bottom ashes, as these are indistinguishable from the olivine of the fluidized bed, the ICP-MS metal content of the olivine was analyzed before and after the gasification process to evaluate the differences.

Results and discussions

Biomass characterization

A preliminary step in the characterization of biomass, produced in contaminated lands and used for energy purposes, consists in the detection of the dispersed contaminants. Here, the first step was to analyze the feedstock used for thermochemical conversion. The characterization of PABR poplar pruning residues, carried out on a dry basis, is reported in Table 4.

These results are close to the data found in literature for similar biomass [6]. The CHNS analysis on poplar pruning residues showed that this biomass can be considered suitable for thermochemical processes as the C/N ratio is greater than 30. The elemental analysis showed a high carbon content, typical of lignocellulosic biomass, that is confirmed by the same high carbon content in the biochar obtained at the end of the gasification process (Table 5). The high carbon content contributes to increase the energy value of the feedstock. The Sulphur content was below the limit of quantification (LOQ) of 0.05% w/w. The analysis of the composition of the overall solid residue (ash + biochar) indicates that the C and H contents are almost half than that of the pure biochar, thus suggesting that ash and biochar fractions are roughly the same.

The analysis of PCBs in biomass samples (summing up all the 31 congeners) indicates an average value equal to 40.47 ng/g. In Table 6 the total concentration (expressed in ng/g) of the only congeners detected in the poplar pruning residues is reported. The PCB Markers were the most abundant congeners, representing the 54% of the total amount of PCBs. Among these six congeners, the n.138 reveals the highest value (8.84 ± 2.04 ng/g). As for the twelve dioxin-like congeners [35], only two were detected with very low concentrations (1.95 ± 0.36 and 1.76 ± 0.16, for the 118 and 105 congeners, respectively). No value was observed for the DX-like congeners 77, 81, 114, 123, 156, 157, 167 and 170. Among the non-DX like congeners, the most abundant was the n.95 with a value of 2.96 ± 0.48 ng/g. Overall, the analysis of PCB content revealed that the characterized PABR biomass samples have low concentrations of these xenobiotics: this is in line with recent studies

Table 7
Metals concentration in PABR biomass compared to Literature data.

	Current PABR biomass	Poplar (Phyllis database)	Vervaeke et al., [26]	Aghaalikhani et al., [28] Poplar	Aghaalikhani et al., [28] PABR
Metal	mg/kg	mg/kg	mg/kg		
Li	0.23	–	–		
B	0.12	6			
Na	10.35	120	–	712	146
Mg	46.11	610	–	29	150
Ca	65.93	2236	–	508	1805
Al	19.07	10	–		
K	458.03	705	–	364	517
Cr	8.82	0.36	4.1 ± 0.8		
Mn	38.77	17	–	1.0	2.3
Fe	47.44	43.84	–		
Co	0.33	–	–		
Ni	**0.99**	**–**	**2.2 ± 0.15**	**70.4**	**35.4**
Cu	4.78	13	6.7 ± 0.6	2.6	2.9
Zn	44.74	34	**150 ± 30**	**30.3**	**64.7**
As	0.17	0.17	–	0.6	0.7
Sr	206.92	169	–	30.3	309.6
Mo	1.03	–	–		
Cd	**8.68**	**0.26**	**3.8 ± 0.3**	**0.4**	**0.4**
Cs	0.02	–	–		
Ba	8.08	–	–		
Pb	**1.52**	**0.7**	**3.5 ± 0.4**	**0.1**	**1.0**
Bi	0.02	–	–		

Fig. 3. Illustration of the bed material before (left) and after (right) the gasification.

which affirm that PCBs do not accumulate in steams and shoots but mainly in the root system [9,36]. For such reasons the PCB are not considered in the successive sections.

Metals assessment

Metals in biomass

Biomass characterization revealed that several metals (potentially harmful) are present in the biomass, such as K, Mn, Zn, Sr, Cd, Pb (see Table 7). It is important to remark that the soil considered in the PABR experiment revealed a high content of Ca and Mg [9,31] and therefore the amount of alkali metals in the biomass is predominant. The data obtained by the analysis of the PABR biomass are compared with the composition of a typical poplar biomass as specified in Phyllis2 database (http://Phyllis.nl), with another contaminated biomass (willow wood) [26] and with literature data reported in the paper of Aghaalikhani et al. [28], in which traditional and contaminated poplar was compared. It is possible to observe that both the contaminated samplings showed high concentration of hazardous component as Ni, Cd, Pb and, Zn in [28] and in [26]. It must be pointed out that, in the current study, the poplar pruning residues were collected only from shoots, which contain lower content of metals than the roots, as shown in previous works [37,38]. Compared to [28], here Ni and Zn have lower concentrations, Cd and Pb have higher concentrations, while Sr concentration is high in both cases. Comparing the current results with those achieved in [26], we can put in evidence that in PABR biomass treated in this work, the Cd and Cr values are considerably greater than those observed by Varveake et al. [26], while the other contaminants show lower concentrations. This is probably because Cd and Cr are present in the original soil [37] and they can translocate in the upper part of the poplar tree. In fact, soil pollutant investigations performed in the poplar recovered area of Southern Italy showed a significant (>1) Translocation Factor (TF), calculated as the ratio of metal concentration in leaves over that in roots, for cadmium [37,38]. The main elements influencing the volatility of metals in the gasification process are K, Mg, Ca, Cl and S [39]. For the configuration of the analytical instruments owned by the laboratory, it was not possible to determine Cl and S.

Table 8
Metal concentration in the olivine bed (mg/kg).

Metal	Original bed	Reacted bed	Difference	Results in [26]
Li	1.21	0.57	−0.64	
B	<LOQ	<LOQ	–	
Na	209.05	146.55	−62.50	
Mg	411213.20	340073.37	−71139.83	
Al	1364.78	592.58	−772.20	
K	22.80	221.23	198.43	
Ca	383.23	240.04	−143.19	
Cr	**246.06**	**287.40**	**41.34**	**22.1**
Mn	1436.45	1169.46	−266.99	
Fe	96771.56	67052.61	−29718.95	
Co	99.40	49.58	−49.82	
Ni	**3257.06**	**2839.48**	**−417.58**	**16.9**
Cu	31.76	32.21	0.45	122.0
Zn	15.29	9.52	−5.77	880.0
Ga	0.16	0.09	−0.07	
As	301.56	874.66	573.10	
Sr	1.45	1.96	0.51	
Ag	0.03	0.03	0.00	
Cd	**0.01**	**0.02**	**0.01**	**10.1**
Ba	0.54	0.51	−0.03	
Tl	<LOQ	<LOQ	–	
Pb	**0.04**	**0.07**	**0.03**	**7.7**

Table 9
Metal content in flying ashes.

Flying ashes	Present case (mg/kg)	Vervaeke [26] (mg/kg)
Li	119.47	
B	816.12	
Na	345.56	
Mg	420.14	
Al	571.00	
K	654.80	
Cr	**58.85**	**13.9**
Mn	164.36	
Fe	315.02	
Ni	**19.37**	**13.9**
Cu	134.47	109
Zn	42.51	1410
Sr	16.07	
Cd	**40.88**	**62.2**
Ba	0.00	
Pb	**76.75**	**22.2**

Table 10
Metal content in fugitive ashes.

Fugitive ashes	Present (mg/m^3)	Vervaeke [26] (mg/kg)
Li	78.25	
B	126.05	
Na	94.82	
Mg	92.15	
Al	92.63	
K	114.63	
Cr	**58.12**	**0**
Mn	98.17	
Fe	405.43	
Ni	–	**12.2**
Cu	123.26	78.6
Zn	606.40	17900.00
Sr	78.39	
Cd	–	**71.9**
Ba	54.46	
Pb	**35.14**	**225.8**

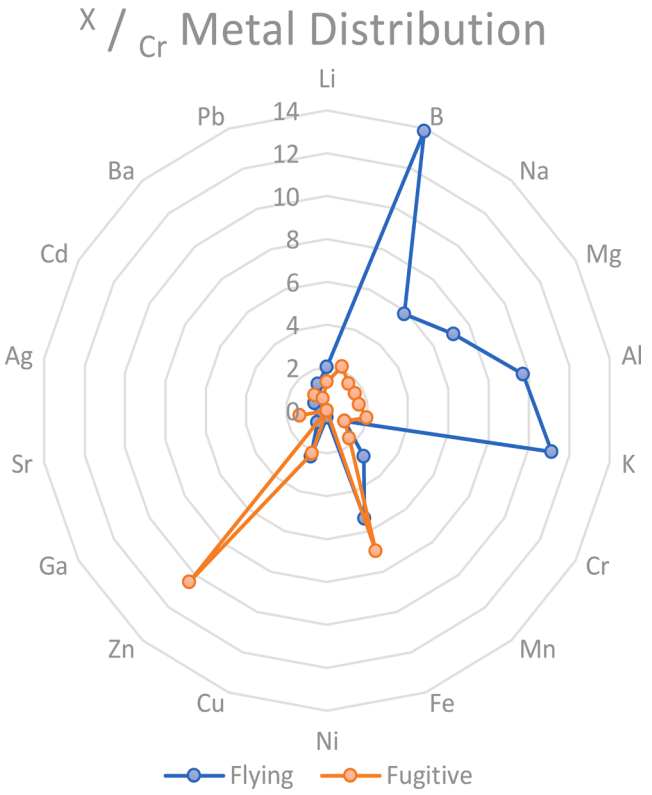

Fig. 4. Comparison of relative metal concentration in the flying and fugitive ashes.

Table 11
Metals concentration in fugitive ashes (3rd bubbler).

Metals	mg/m^3	% of fugitive
Li	0.03	0.04%
B	2.13	1.69%
K	3.50	3.05%
Cr	0.12	0.21%
Pb	0.09	0.26%

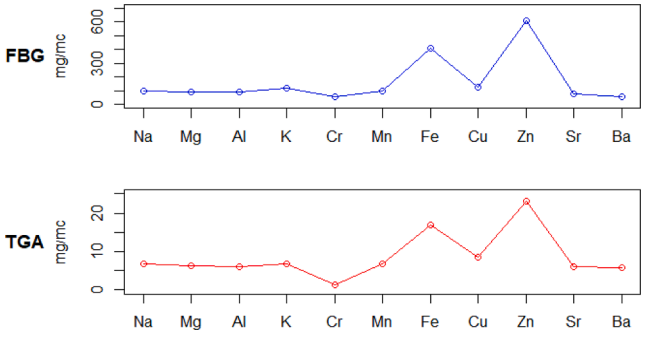

Fig. 5. Metal concentration in fugitive ashes in FBG and in TGA-DTA processes [45].

Table 12
VOCs observed in syngas.

VOC	Before Filter (mg/m^3)	After Filter (mg/m^3)	Reduction %
Benzene	0.792	0.581	26.7
Toluene	1.326	0.705	46.9
Ethylbenzene	0.152	0.027	82.3
m, p – Xylene	0.210	0.182	13.5
o – Xylene	0.206	0.176	14.5
Styrene	0.704	0.584	17.1

Table Ia
VOCs before ceramic filter.

Propene	Benzoic acid, methyl ester
1,3-Butadiene	1,4-Dihydronaphthalene
1-Buten-3-yne	Benzofuran, 3-methyl-
1,2-Butadiene	Benzonitrile, 4-methyl-
1,3-Cyclopentadiene	Benzene, 1,4-diethenyl-
Benzene	2-Methylindene
2-Butenedinitrile	Benzene, (1-methyl-2-cyclopropen-1-yl)-
Thiophene	Benzene, 1-butynyl-
Acetic acid	Naphthalene
Toluene	1,4-Dihydronaphthalene
Formamide	Azulene
Pyridine, 2-methyl-	1,2-Naphthalenedione
Benzene, chloro-	Benzo[b]thiophene
Ethylbenzene	Benzene, 1-pentynyl-
Benzene, 1,3-dimethyl-	Quinoxaline
Pyridine, 3-methyl-	Quinoline
Phenylethyne	Naphthalene, 2-methyl-
1,3,5,7-Cyclooctatetraene	1H-Inden-1-one, 2,3-dihydro-
Butanedioic acid, phenyl-	Indole
Styrene	Biphenyl
Pyridine, 2-ethenyl-	1,1′-Biphenyl, 2-methyl-
Phenol	Naphthalene, 2-ethyl-
Benzene, 1-propynyl-	Naphthalene, 2,6-dimethyl-
Benzaldehyde	Biphenylene
Benzene, 1-ethenyl-4-methyl-	Naphthalene, 2-ethenyl-
Benzene, cyclopropyl-	Diphenylmethane
Benzofuran	1,1′-Biphenyl, 4-methyl-
Benzonitrile	Acenaphthene
Indane	Dibenzofuran
Benzyl Alcohol	2-Naphthalenecarbonitrile
Acetophenone	Fluorene
Benzonitrile, 2-methyl-	2-Hydroxyfluorene

Metals in FBG and in syngas

The distribution of pollutants among the streams generated by the gasification process is extremely important for assessing a safe separation and disposal process. The metal particles are concentrated in the solid fractions, which can be divided into 3 types: *bottom, flying and fugitive ashes*, depending on the stream they are associated with. The bottom ashes, including the char, are the heaviest ones, and they remain inside the gasification chamber. This means that the analysis of such components must take in account the presence (and the possible interaction) of olivine. The flying ashes are volatile enough to be transported by the generated syngas and are captured by the cyclone.The fugitive ashes are captured by the trapping system (using bubblers) placed downstream from the ceramic filter. Admittedly, such classification should also consider the effect of metal volatility [9,10] but the analysis of the different gaseous compounds generated by the same component is out of the scope of the present paper and such analysis is here discarded. From the comparison between the metals contained in the reactor bed at the end of the gasification, and in the olivine used as bed material (see also Fig. 3), it is possible to evaluate the deposit of bottom ashes and, according to a previous work [40], the syngas contamination due to the release of volatile metals from the olivine. Pushp et al. [41], investigated the influence of olivine on the formation of gaseous alkali compounds by using a FBG with double chamber, and by operating ratio among steam/air and biomass that are similar to the analysis carried out here. The papers demonstrated that the olivine helps in reducing condensable tars in the syngas (as also confirmed by the studies in [22;27]). However, the authors do not cite the variation of olivine properties during the process and this leaves a relevant research question that it is worth to be investigated here. In Table 8, the difference in the bed material metal concentration before and after the gasification process is reported. Where the variation (Δ) is positive, the quantity of metal contained in the biomass and deposited at the bottom of the reactor exceeds the eventual release of the same metal from the olivine. On the opposite, a negative Δ indicates that the metal emission from the olivine is predominant over deposit. This consequently affects the metal concentration in the flying and fugitive ashes. In particular, here it is worth to analyse the fate of the heavy metals previously identified and to compare them with the results in [26] where a similar analysis was carried out on different configurations (different biomass - willow - and a different gasification strategy - downdraft) to examine the occurrence of common features. Cd and Pb content in olivine does not change much, while we noticed a large variation in Ni (released) and Cr (deposited). It is also interesting to notice that, among other components, large quantities of Mg and Fe are released from the bed. This was expected, due to the composition of olivine that is very rich in these two metals. Such

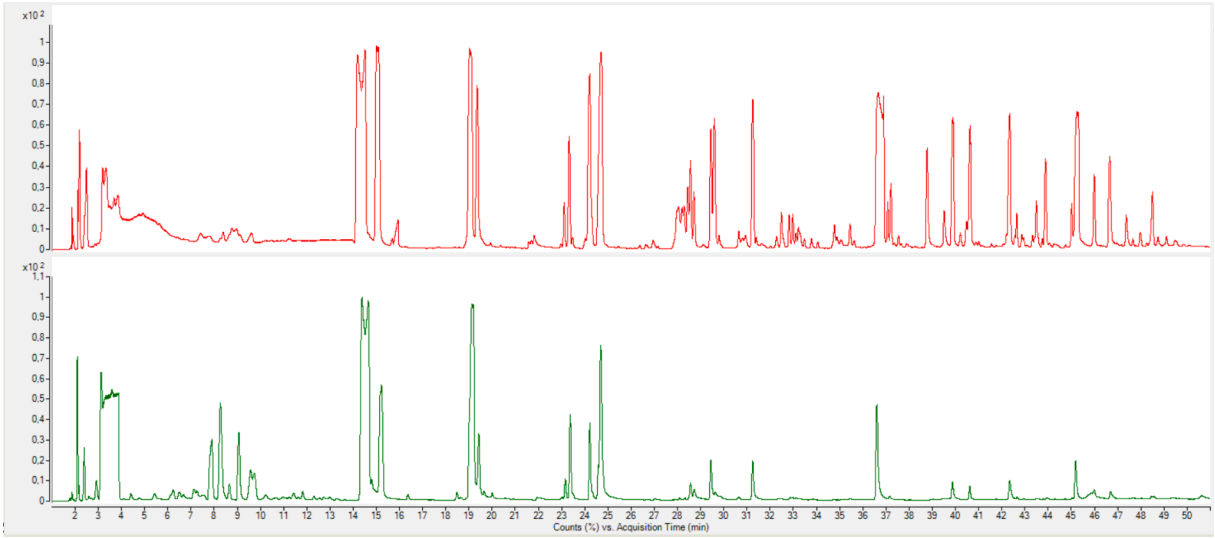

Fig. 6. VOCs chromatograms measured before (red) and after (green) the ceramic filter.

Table Ib
VOCs after ceramic filter.

Propene	Benzene
Propyne	Thiocyanic acid, methyl ester
2-Butene, (E)-	Cyclotrisiloxane, hexamethyl-
2-Pentene	Toluene
2-Butyne	Thiophene, 3-methyl-
1,4-Pentadiene	Pyridine, 2-methyl-
Furan	Ethylbenzene
Acetone	Benzene, 1,3-dimethyl-
1,4-Pentadiene	Phenylethyne
Acetonitrile	Styrene
Methyl isocyanide	Benzene, 1-ethenyl-2-methyl-
1,3-Cyclopentadiene	Benzene, cyclopropyl-
2-Propenenitrile	Benzofuran
Hexane	Benzonitrile
3-Pentanone	Benzene, 1-propynyl-
1,3-Cyclopentadiene	Naphthalene
Benzene, 1,3,5-trifluoro-	Benzo[b]thiophene
Propanenitrile	Naphthalene, 1-methyl-
2-Propenenitrile, 2-methyl-	Biphenyl
1,3-Cyclopentadiene, 1-methyl-	Biphenylene
2-Butenedinitrile, (E)-	Acenaphthene
2-Butenenitrile	Dibenzofuran

circumstance was already analysed in the paper of Serrano et al. [42], that studied the FBG of *Cynara Cardunculus*, by using olivine and magnesite as bed materials.They noticed a relevant release of Mg, Fe and Cr from the bed. However they did not measure the metal concentration in the bottom ashes and then the extent of their analysis remained limited. The effect of the bed materials in affecting the contaminants content in syngas is often underestimated in the literature [40]. The comparison with the results of [26] can give further useful hints, even if the findings are quite different. In fact in our experiments, only Cr has a similar behaviour, as it is the only metal that is partially deposited among the ones considered in [26] also.

As told, downstream from the reactor, metals were also sampled to determine their presence in the cyclone (flying) ashes or their dispersion in the syngas (fugitive). The flying ashes were collected, mineralised and analised (Table 9), while the fugitive ashes were quantified in relation to the volume of syngas that passed through the trapping bubblers.

In the present analysis, Cd and Ni are almost completely captured by the cyclone filter, and their content is negligible in the fugitive ashes. This result agrees only partially with a recent review about the assessment of HM during gasification process [43] in which it is shown how Cd and Ni have opposite behaviours: the first is easily transported away by the syngas, while the second tends to accumulate mainly in the bottom ash. In the case studied the olivine has influenced the emission of Ni, but the cyclone has represented an effective system of abatement for the fractions in which both Ni and Cd have concentrated. Cr (mainly) and Pb are present in the flying ash, but also in the fugitive demonstrating that the cyclone allows to trap them only in part. Zn released from the olivine is present in both the flying and fugitive ashes, thus posing a serious question on the use of olivine as bed material. As for [26], the metals concentration in the flying ashes is comparable with our values apart from Zn, that has strong concentration in the original biomass also. Zn and Pb are present both in flying and in fugitive ashes. This circumstance is consistent with Cui et al. [44], according to which the volatilization rate of Zn and Pb increased after 700 °C. Comparisons with the results present in the fugitive ashes is more difficult, as in Table 10 the concentrations are expressed in parts per volume (fugitive ashes), while the reference data are reported in ppm. However it is possible to draw some considerations: a) differently from our case, Cr is not present while large Cd quantities are measured; b) Zn, Pb and Cu fractions indicate that in both cases the cyclone is not sufficient to capture them. Trying to find a proper evaluation of the metal distribution among the flying (in mg/kg) and the fugitive ashes (in mg/m^3), the data was normalised with respect to the content in one metal. Cr was chosen as it is present in both the flying (58.85 mg/kg) and in fugitive ash (58.12 mg/m^3). It is then interesting to compare its concentration with the other metals ones to assess a relative variation. The comparison between the relative metal distribution in flying and fugitive ashes is summarised in Fig. 4, where Cr is always equal to 1.

Table Ic
VOCs observed on TGA-DTA sample.

Propene	Oxalic acid, butyl propyl ester
Cyclopropane	Furan, 3-methyl-
Silane, difluorodimethyl-	Acetic acid, methoxy-
Methane, chloro-	Methyl propionate
Glycidol	Benzene
Furan	Propanoic acid
Acetone	Furan, 2,5-dimethyl-
Acetonitrile	Toluene
Acetic acid, methyl ester	3-Furaldehyde

As it can be seen in Fig. 4, most of the metals, i.e. B, Na, Mg, Al, K, Cr, Mn, are contained in the ashes collected by the cyclone. In the fugitive ash only Fe and Zn have a significant concentration, compared to Cr concentration. The reason for the dominant presence of Zn in the fugitive ashes can be explained with the circumstance that such metal has an intermediate-high volatility class (IIb-c in [9]) and then it could be present in the volatile ashes up to the bubbler trap. On the other hand, the concentration of fugitive ashes is very small and then the effective concentration of Fe and Zn is almost negligible. B has an extremely high concentration compared to the low concentrations in biomass and olivine: it is extremely probable that its presence is due to plant criticalities rather than to biomass.The data relative to the fugitive ashes were obtained by analysing only the first 2 bubblers, as the 3rd is used only for testing the effective capability of the metals to be realeased in the enviroment. The only metals also found in the third bubbler (in traces) are showed in Table 11. Their concentration is pratically negligible.

The metal distribution in the ashes or the syngas is very important as it could allow the determination of the proper treatments (guidelines or best practices) to be used for the cleaning of char and/or gaseous compounds produced from thermochemical treatment of PABR biomass based on contamination. To assess a fast procedure to determine the fate of contaminants, the metal distribution measured in the FBG is compared with the results obtained in the TGA-DTA analysis early introduced. TGA-DTA was selected for its capability to rapidly perform a large number of tests and to control the relevant parameters. Even though the tests are carried out with different temperature ranges (here a constant Δ T ramp is used, while in the FBG a constant T is maintained) and thermochemical reaction (here pyrolysis instead of gasification), the authors' guess was that the fate of the contaminants could be similar. Therefore, establishing a correlation between FBG and TGA is highly attractive.

By comparing the TGA-DTA and the FBG emissions, an important result is obtained. The two methodologies have different characteristics as in TGA-DTA there is a small and defined quantity of matrix whose emissions are distributed over a high flow, while in the FBG plant there is a continuous supply of biomass. Furthermore, in FBG, the release of metals from olivine can alter the metal concentration in the syngas and ashes. Although the concentrations are obviously different, the ratios that bind the individual metals are similar (Fig. 5). It is observed that Fe, Cu and Zn, which are the metals expected to be conveyed in the fugitive ash have similar distribution in FGB and TGA-DTA and the overall emissive trend follows roughly the same profile. This result can be considered encouraging and it suggests carrying out successive investigations on a such small case test bench, to preliminary assess possible alternatives.

VOC analysis

Gasifier

The sampling was carried out before and after the ceramic filter. Positively, the filter is operated at a temperature of 400 °C and it is expected that the passage through this porous device at high temperature can have a relevant impact in terms of VOCs reforming. The quantification of BTEXS (Benzene, Toluene, Ethylbenzene, Xylenes and Styrene) are reported in Table 12 to evaluate the quality of syngas and the efficiency of the ceramic filter.

The filter demonstrated to be very effective in reducing the VOCs quantity, especially about the most complex (and poisoning) components. A qualitative analysis was also conducted on the VOCs concentration before and after the ceramic filter, by using GC/MS system. The chromatograms shown in Fig. 6 indicate that the count of heaviest and more toxic compounds, located in the right side of the plot, is significantly reduced after the passage in the heated filter, where the high temperature can support the tar cracking. This is also confirmed by the list of the measured VOCs, indicating that 64 compounds were identified in the syngas stream before the filter. After the filter the number of compounds drops to 44 only. The list of VOCs is reported in Appendix I (Table I.a and I.b). As expected, the number of analytes with a lower molecular weight (in the C3-C6 range) increases after the ceramic filter, while the number of heavier compounds decreases. This phenomenon confirms the conjecture that the heated ceramic filter fragments the heaviest molecules into smaller ones. Some of the lightest PAHs (es. Naphthalene, Fluorene, Biphenylene, etc.) also appeared. VOCs are generated from incomplete combustion phenomena of carbonaceous matrix [46] and, by comparing the analytes identified in the TGA-DTA (Table I.c) with those determined in the real FBG plant, some interesting analogies and differences can appear. As expected, in the real plant a higher number of VOCs are obtained. This circumstance is a consequence of the fact that the VOCs obtained in TGA-DTA are generated in ideal conditions. When the process is on a real FBG, complex VOCs recombine, interacting with the system materials and producing a series of other compounds, that are characteristics of the real systems. A confirmation of this is given by Furan: this analyte is largely present in the TGA VOCs, while it is absent in the FBG syngas. However, many furan-based compounds have been identified (Benzofuran; Benzofuran, 3-methyl-; Dibenzofuran, etc.). In the post filter syngas, the thermo-catalytic effect of the filter leads to a fragmentation of the larger molecules (eg. Fluorene, Naphthalene-based compounds, etc.) into smaller molecules, so generating Furan. However, some of the VOCs determined in TGA-DTA are present in the syngas analyzed before the filter (Propene, Benzene, Toluene) and the agreement is also closer in the post filter syngas (propene, furan, acetone, acetonitrile, benzene, toluene).

Conclusions

The present study was aimed to assess the technical feasibility of PABR biomass production as an integrated and sustainable strategy for producing renewable energy while depolluting contaminated soils in an industrial symbiosis framework. In this work was conducted, for the first time to the knowledge of the authors, an in-depth and complete investigations lab-scale and prototype scale to evaluate the fate of contaminants in the process of gasification of contaminated biomass. The viability of using PABR biomass in gasification plants was experimentally analyzed. After characterizing PABR biomass (contaminants assessment, etc.), the concentration of VOCs and the metals released from the gasification process were measured using a wide set of analyses including TGA-DTA, VOCs analysis and metal sampling. It was demonstrated that no significant PCB content is observed in the biomass due to the degradation process occurring in the rhizosphere. Heavy metals released from the wood matrix during the gasification process mostly concentrate in the ashes, while the metals detected in the syngas and measured by the instruments, represent only a portion of the total amount of those originally occurred in the poplar pruning residues. The analysis in the FBG treatment demonstrated that the different metals show different concentration in the bottom (and flying) and in the fugitive ashes because of some properties, such as volatilization. Furthermore, the olivine itself releases metals that mix with the HMs present in the biomass increasing their overall content and the needs to clean the syngas before using it for energy purposes. However, it is important to notice that most of the metals were concentrated on bottom and flying ashes, while only a minor fraction (that was almost completely trapped in the bubbling bottles) was detected in the fugitive ashes. Furthermore, comparisons among metals concentration in FBG and TGA-DTA suggest that the fate of the elements is similar. As for the VOCs, their quantity is limited, and the presence of catalytic filter allows to abate the contents of the heavier compounds. Even in this case, the TGA-DTA returns VOCs that are qualitatively similar to the VOCs detected in the syngas.

It is thus possible to conclude that:

a) This analysis is unique in treating FBG of contaminated biomass also considering the metal emissions from biomass as well as the release from the bed material.
b) It is possible to identify the metal distribution and the VOCs composition and then to set up properly the cleaning processes.
c) With some precautions, the TGA-DTA can be preliminarily used to identify the metals that should be present in the ashes, the char or in the syngas, similarly to what happens in a real gasification process.
d) The wide application of PABR not only represents a sustainable treatment of contaminated soils, but it is also an interesting source of renewable energy, supporting the reduction of global emissions.

Declaration of Competing Interest

The authors declare that they have no known competing financial interests or personal relationships that could have appeared to influence the work reported in this paper.

Acknowledgments

This research was financially supported by a project entitled “Biorimedio fitoassistito: una strategia verde per il recupero di aree contaminate e la valorizzazione di biomassa – SOLUZIONI VERDI”, funded by the Apulia Region, Italy (POR PUGLIA FESR-FSE 2014-2020, Azione 1.6. Avviso “Innonetwork”, project code Q3ITQH5) and was supported by the Italian Ministry of Agricultural, Food and Forestry Policies (MiPAAF) under the AGROENER project (D.D. n. 26329, 1 April 2016) - http://agroener.crea.gov.it/.

The authors would like to thank Giorgia Aimola (IRSA-CNR) for her precious help in performing PCB chemical analysis.

Appendix I

Tables Ia–Ic.

References

[1] International Energy Agency I. Market Report Series: Renewables 2018.
[2] Mueller SA, Anderson JE, Wallington TJ. Impact of biofuel production and other supply and demand factors on food price increases in 2008. Biomass Bioenergy 2011;35(5):1623–32.
[3] Pulford ID, Watson C. Phytoremediation of heavy metal-contaminated land by trees – a review. Environ Int 2003;29. https://doi.org/10.1016/S0160-4120(02)00152-6.
[4] ISPRA. Contaminated sites of national interest (SIN) 2014. https://www.isprambiente.gov.it/en/activities/soil-and-territory/copy_of_contaminated-sites/contaminated-sites-of-national-interest-sin (accessed June 7, 2022).
[5] Feng N-X, Yu J, Zhao H-M, Cheng Y-T, Mo C-H, Cai Q-Y, et al. Efficient phytoremediation of organic contaminants in soils using plant–endophyte partnerships. Sci Total Environ 2017;583:352–68.

[6] Ruttens A, Boulet J, Weyens N, Smeets K, Adriaensen K, Meers E, et al. Short rotation coppice culture of willows and poplars as energy crops on metal contaminated agricultural soils. Int J Phytorem 2011;13(sup1):194–207.
[7] Giudicianni P, Pindozzi S, Grottola CM, Stanzione F, Faugno S, Fagnano M, et al. Pyrolysis for exploitation of biomasses selected for soil phytoremediation: characterization of gaseous and solid products. Waste Manage 2017;61:288–99.
[8] Fiorentino N, Ventorino V, Rocco C, Cenvinzo V, Agrelli D, Gioia L, et al. Giant reed growth and effects on soil biological fertility in assisted phytoremediation of an industrial polluted soil. Sci Total Environ 2017;575:1375–83.
[9] Ancona V, Barra Caracciolo A, Campanale C, De Caprariis B, Grenni P, Uricchio VF, et al. Gasification treatment of poplar biomass produced in a contaminated area restored using plant assisted bioremediation. J Environ Manage 2019;239:137–41.
[10] Nzihou A, Stanmore B. The fate of heavy metals during combustion and gasification of contaminated biomass-A brief review. J Hazard Mater 2013:256–7. https://doi.org/10.1016/j.jhazmat.2013.02.050.
[11] Keller C, Ludwig C, Davoli F, Wochele J. Thermal treatment of metal-enriched biomass produced from heavy metal phytoextraction. Environ Sci Technol 2005;39 (9):3359–67.
[12] van Ginneken L, Meers E, Guisson R, Ruttens A, Elst K, Tack FMG, et al. Phytoremediation for heavy metal-contaminated soils combined with bioenergy production. J Environ Eng Landscape Manage 2007;15. https://doi.org/10.1080/16486897.2007.9636935.
[13] Chalot M, Blaudez D, Rogaume Y, Provent A-S, Pascual C. Fate of trace elements during the combustion of phytoremediation wood. Environ Sci Technol 2012;46 (24):13361–9.
[14] Al Chami Z, Amer N, Smets K, Yperman J, Carleer R, Dumontet S, et al. Evaluation of flash and slow pyrolysis applied on heavy metal contaminated Sorghum bicolor shoots resulting from phytoremediation. Biomass Bioenergy 2014;63:268–79.
[15] Giudicianni P, Pindozzi S, Grottola CM, Stanzione F, Faugno S, Fagnano M, et al. Effect of feedstock and temperature on the distribution of heavy metals in char from slow steam pyrolysis of contaminated biomasses. Chemical. Engineering Transactions 2017;58. https://doi.org/10.3303/CET1758085.
[16] Grottola CM, Giudicianni P, Pindozzi S, Stanzione F, Faugno S, Fagnano M, et al. Steam assisted slow pyrolysis of contaminated biomasses: effect of plant parts and process temperature on heavy metals fate. Waste Manage 2019;85:232–41.
[17] Grottola CM, Giudicianni P, Michel JB, Ragucci R. Torrefaction of woody waste for use as biofuel. Energy Fuels 2018;32(10):10266–71.
[18] Borello D, Venturini P, Rispoli F, Rafael SGZ. Prediction of multiphase combustion and ash deposition within a biomass furnace. Appl Energy 2013;101:413–22.
[19] Borello D, Cedola L, Frangioni GV, Meloni R, Venturini P, De Filippis P, et al. Development of a numerical model for biomass packed bed pyrolysis based on experimental validation. Appl Energy 2016;164:956–62.
[20] Borello D, Pantaleo A, Caucci M, De Caprariis B, De Filippis P, Shah N. Modeling and experimental study of a small scale olive pomace gasifier for cogeneration: energy and profitability analysis. Energies 2017;10(12):1930.
[21] McKendry P. Energy production from biomass (part 3): Gasification technologies. Bioresour Technol 2002;83(1):55–63.
[22] Kuba M, Skoglund N, Öhman M, Hofbauer H. A review on bed material particle layer formation and its positive influence on the performance of thermo-chemical biomass conversion in fluidized beds. Fuel 2021;291:120214.
[23] Rapagnà S, Jand N, Kiennemann A, Foscolo PU. Steam-gasification of biomass in a fluidised-bed of olivine particles. Biomass Bioenergy 2000;19. https://doi.org/10.1016/S0961-9534(00)00031-3.
[24] Devi L, Ptasinski KJ, Janssen FJJG, van Paasen SVB, Bergman PCA, Kiel JHA. Catalytic decomposition of biomass tars: Use of dolomite and untreated olivine. Renewable Energy 2005;30(4):565–87.
[25] Constantinou DA, Fierro JLG, Efstathiou AM. A comparative study of the steam reforming of phenol towards H2 production over natural calcite, dolomite and olivine materials. Appl Catal B 2010;95(3-4):255–69.
[26] Vervaeke P, Tack FMG, Navez F, Martin J, Verloo MG, Lust N. Fate of heavy metals during fixed bed downdraft gasification of willow wood harvested from contaminated sites. Biomass Bioenergy 2006;30(1):58–65.
[27] Di Carlo A, Borello D, Sisinni M, Savuto E, Venturini P, Bocci E, et al. Reforming of tar contained in a raw fuel gas from biomass gasification using nickel-mayenite catalyst. Int J Hydrogen Energy 2015;40(30):9088–95.
[28] Aghaalikhani A, Savuto E, Di Carlo A, Borello D. Poplar from phytoremediation as a renewable energy source: Gasification properties and pollution analysis. Energy Procedia 2017;142:924–31.
[29] Mitsuoka K, Hayashi S, Amano H, Kayahara K, Sasaoaka E, Uddin MA. Gasification of woody biomass char with CO2: the catalytic effects of K and Ca species on char gasification reactivity. Fuel Process Technol 2011;92(1):26–31.
[30] Li C, Hirabayashi D, Suzuki K. A crucial role of O2- and O22- on mayenite structure for biomass tar steam reforming over Ni/Ca12Al14O33. Appl Catal B 2009;88(3-4): 351–60.
[31] Ancona V, Barra Caracciolo A, Grenni P, Di Lenola M, Campanale C, Calabrese A, et al. Plant-assisted bioremediation of a historically PCB and heavy metal-contaminated area in Southern Italy. New Biotechnol 2017;38:65–73.
[32] Gallucci F, Liberatore R, Sapegno L, Volponi E, Venturini P, Rispoli F, et al. Influence of oxidant agent on syngas composition: gasification of hazelnut shells through an updraft reactor. Energies 2019;13(1):102.
[33] Littlewood K. Gasification: theory and application. Prog Energy Combust Sci 1977; 3(1):35–71.
[34] Yang H, Yan R, Chen H, Lee DH, Zheng C. Characteristics of hemicellulose, cellulose and lignin pyrolysis. Fuel 2007;86(12-13):1781–8.
[35] Ahlborg UG, Hanberg A. Toxic equivalency factors for dioxin-like PCBs. Environ Sci & Pollut Res 1994;1(2):67–8.
[36] Jou J-J, Chung J-C, Weng Y-M, Liaw S-L, Wang MK. Identification of dioxin and dioxin-like polychlorbiphenyls in plant tissues and contaminated soils. J Hazard Mater 2007;149(1):174–9.
[37] Ancona V, Caracciolo AB, Campanale C, Rascio I, Grenni P, Di Lenola M, et al. Heavy metal phytoremediation of a poplar clone in a contaminated soil in southern Italy. J Chem Technol Biotechnol 2020. https://doi.org/10.1002/jctb.6145.
[38] Ancona V, Rascio I, Aimola G, Campanale C, Grenni P, Lenola MD, et al. Poplar-assisted bioremediation for recovering a PCB and heavy-metal-contaminated area. Agriculture 2021;11(8):689.
[39] Chai Y, Bai Ma, Chen A, Peng L, Shao J, Shang C, et al. Thermochemical conversion of heavy metal contaminated biomass: Fate of the metals and their impact on products. Sci Total Environ 2022;822:153426.
[40] Gallucci F, Palma A, Vincenti B, Carnevale M, Paris E, Ancona V, et al. Fluidized bed gasification of biomass from plant assisted bioremediation (PABR): Lab-scale assessment of the effect of different catalytic bed material on emissions. Fuel 2022; 322:124214.
[41] Pushp M, Gall D, Davidsson K, Seemann M, Pettersson JBC. Influence of bed material, additives, and operational conditions on alkali metal and tar concentrations in fluidized bed gasification of biomass. Energy Fuels 2018;32(6): 6797–806.
[42] Serrano D, Kwapinska M, Sanchez-Degado S, Leahy JJ. Ash properties from cynara cardunculus L. Gasification. European Biomass Conference and Exhibition Proceedings, vol. 2016, 2016.
[43] Raheem A, He Q, Mangi FH, Areeprasert C, Ding Lu, Yu G. Roles of heavy metals during pyrolysis and gasification of metal-contaminated waste biomass: a review. Energy Fuels 2022;36(5):2351–68.
[44] Cui X, Shen Ye, Yang Q, Kawi S, He Z, Yang X, et al. Simultaneous syngas and biochar production during heavy metal separation from Cd/Zn hyperaccumulator (Sedum alfredii) by gasification. Chem Eng J 2018;347:543–51.
[45] Borello D, de Caprariis B, Ancona V, Paris E, Plescia P, Gallucci F. Use of an innovative TGA apparatus for sampling the emissions generated by pyrolysis of plant assisted bio-remediation biomass. European Biomass Conference and Exhibition Proceedings, 2020.
[46] Paris E, Carnevale M, Vincenti B, Palma A, Guerriero E, Borello D, et al. Evaluation of VOCs emitted from biomass combustion in a small CHP plant: difference between dry and wet poplar woodchips. Molecules 2022;27(3):955.